The Time-Domain Cell Method Is a Coupling of Two Explicit Discontinuous Galerkin Schemes With Continuous Fluxes

Bernard Kapidani[1], Lorenzo Codecasa[2], and Ruben Specogna[3]

[1]Institute for Analysis and Scientific Computing, Technische Universität Wien, 1040 Vienna, Austria
[2]Dipartimento di Elettronica, Informazione e Bioingegneria, Politecnico di Milano, 20133 Milan, Italy
[3]Dipartimento Politecnico di Ingegneria ed Architettura, University of Udine, 33100 Udine, Italy

The cell method (CM) or discrete geometric approach (DGA) in the time domain, already introduced by Codecasa *et al.* in 2008 for the coupled Ampere–Maxwell and Faraday equations, is here recast as a Galerkin Method similar to the finite-element method (FEM). In particular, it is shown to be a mixed method comprising an explicit scheme and two discontinuous Galerkin (DG) FEM spaces formulated on dual meshes, in which each of the two function spaces provides a continuous numerical flux choice for its dual mesh counterpart. The implemented version is shown to compare favorably in terms of accuracy and efficiency with respect to the classic conforming FEM scheme using Whitney elements. When tested on the same tetrahedral mesh, the Courant–Friedrichs–Lewy (CFL) condition for the proposed approach is a factor of 2 less restrictive on the time step with respect to the curl-conforming FEM scheme.

***Index Terms*— Discontinuous Galerkin (DG), explicit time-stepping, finite difference in time-domain (FDTD), time-domain Maxwell, unstructured grids.**

I. Introduction

FOR time-dependent problems in high-frequency electromagnetics, the finite difference in time-domain (FDTD) method [1] is arguably the most long lived and ubiquitous numerical method available in the literature. Nevertheless, when solving problems that present curved interfaces between different materials, it is natural to seek a numerical method that works well on an unstructured grid (usually a simplicial one, given the abundance of mesh generators in such case).

In this setting, the use of curl conforming, edge element based [2], formulations within the finite-element method (FEM) is a common practice in the computational electromagnetics (CEM) community. Numerical time-stepping schemes based on said finite elements involve inverting large sparse mass matrices which, due to the support of the basis functions, are banded but not block diagonal, making the inverse a fully populated matrix (in general). This matrix inversion becomes rapidly unfeasible as the size of the problem to be solved increases. The common choice is rather to solve the linear system iteratively at every time step, using a conjugate gradient (CG) solver (the mass matrix is symmetric positive definite), which preserves the sparsity of the system, but involves several matrix–vector product operations per time step to converge. Moreover, if one is interested in both electric- and magnetic-field values, an additional issue is that one of the two fields is approximated by polynomials of one degree lower than the maximum, which fact bounds the total order of accuracy of the method [3].

To avoid these issues, alternative FEM formulations based on completely discontinuous basis functions have been more recently explored, in which the basis functions for both fields are piecewise polynomials (of arbitrarily high degree) whose support is restricted to a single element, the so-called discontinuous Galerkin (DG) FEM. The DG approach does provide naturally block-diagonal mass matrices, but the resulting global function space in which the numerical solution lives is clearly much larger than the physically meaningful one, and nonphysical solutions do indeed appear, which are called spurious modes in the literature. The general recipe to recover a reliable numerical solution hinges (see [4] and references therein) then on a combination of the following: artificial numerical energy dissipation, (often unreasonably) high degree in the approximating polynomials, and the introduction of additional unknowns living on the skeleton of the mesh with fine-tuned penalty parameters (mesh size and polynomial degree dependent).

A recent alternative road to the solution of the matter, introduced by Codecasa and Politi [7] as a kind of explicit-in-time finite-integration technique (FIT [8]) on tetrahedral meshes, has been further developed by Codecasa *et al.* [9], [10]. This latter approach is theoretically rooted in the cell method (CM, see [5]), alternatively called a discrete geometric approach (DGA, see [6]). This method is, in the authors' opinion, not well understood till date, as it shares both properties from the family of finite-volume methods (its reliance on conservative flux variables) and from the FEM (its use of basis functions defined in a piecewise fashion to approximate the unknown fields).

The present contribution aims at formally recasting this method for the numerical solution of the time-dependent Maxwell equations as the DG FEM method and in passing shed some more light on its main advantageous properties. In Section II, the basic CM terminology and the rationale of the method are recalled. In Sections III and IV, the novel DG-FEM spaces and weak forms for the discrete system of equations are given. Section V presents the numerical results which show the performance of the given method in comparison with the known FDTD and FEM approaches.

Manuscript received August 18, 2019; revised October 7, 2019; accepted November 1, 2019. Date of current version December 20, 2019. Corresponding author: B. Kapidani (e-mail: bernard.kapidani@tuwien.ac.it).

Color versions of one or more of the figures in this article are available online at http://ieeexplore.ieee.org.

Digital Object Identifier 10.1109/TMAG.2019.2952015

0018-9464 © 2019 IEEE. Personal use is permitted, but republication/redistribution requires IEEE permission.
See http://www.ieee.org/publications_standards/publications/rights/index.html for more information.

Authorized licensed use limited to: University of Udine. Downloaded on January 25,2021 at 10:40:43 UTC from IEEE Xplore. Restrictions apply.

Concluding remarks and hints at future work directions are given in Section VI.

II. Abstract Cell Method Formulation

We aim to approximate, via the CM, the time-dependent Ampère–Maxwell and Faraday equations

$$\varepsilon \partial_t \boldsymbol{e}(\boldsymbol{r}, t) = \nabla \times \boldsymbol{h}(\boldsymbol{r}, t) \tag{1}$$

$$\mu \partial_t \boldsymbol{h}(\boldsymbol{r}, t) = -\nabla \times \boldsymbol{e}(\boldsymbol{r}, t) \tag{2}$$

to be solved $\forall t \in [0, +\infty)$ and for each $\boldsymbol{r}$ in the bounded domain $\Omega \subset \mathbb{R}^{2,3}$. For simplicity of presentation, we consider the source-free equations with time invariant materials. If the initial conditions for the electric field $\boldsymbol{e}(\boldsymbol{r}, 0)$ and the magnetic field $\boldsymbol{h}(\boldsymbol{r}, 0)$ are such that the electromagnetic Gauss laws are also satisfied, the solution of (1) and (2) will satisfy all four Maxwell equations for all times t.

The CM [5] is based on the use of two dual meshes: a primal simplicial mesh (i.e., triangular, tetrahedral) as in the FEM, and a polytopal one which is the barycentric dual of the primal grid. There are standard procedures by which we assign to each d-dimensional geometric entity of the mesh an (D-d)-dimensional entity in the dual mesh (see [5], [6]). In the CM approximation, naturally formulated in $D = 3$ dimensions, the discrete degrees of freedom (DoFs) are chosen *a priori* to be line integrals of the unknown $\boldsymbol{e}$ and $\boldsymbol{h}$ fields on primal and dual mesh edges, respectively. We denote them by column vectors $\mathbf{u}$ and $\mathbf{f}$. The curl operators on the r.h.s. of (1) and (2) are written in integral form by using Stokes' theorem on each primal and dual facet plus the definition of the DoFs. They are thus naturally encoded by the edge-to-facet incidence matrix $\mathbf{C}$ and its transpose $\mathbf{C}^T$. To have a complete equivalent of the continuous system of integral equations, mappings between line integrals on primal [dual] edges and fluxes on [primal] dual facets must be constructed, sometimes called Hodge star operators [11], which act as a discrete geometric counterpart of the material tensors

$$\mathbf{M}_\varepsilon \partial_t \mathbf{u} = \mathbf{C}^T \mathbf{f} \tag{3}$$

$$\mathbf{M}_\mu \partial_t \mathbf{f} = -\mathbf{C}\mathbf{u} \tag{4}$$

where the form of square matrices $\mathbf{M}_\mu$, $\mathbf{M}_\varepsilon$ depends on the analytic form of the material tensor and on the geometric properties of the mesh. In [7], a procedure to obtain block diagonal (hence, cheaply invertible) matrices for these operators was developed for the first time.

III. Mesh and Approximation Spaces

We wish to show that the system of ordinary differential equations in (3) and (4) is the coupling of two DG-FEM schemes with continuous fluxes. To show this, we assume a starting shape-regular triangulation (i.e., a simplicial complex) for Ω and proceed as follows: take each mesh element T, compute its centroid, and connect it via a segment to the barycentra of the facets in its boundary (denoted ∂T). Successively, take the edges on the boundary of each facet of T and connect the centroid of the given facet to all barycentra of said edges. Finally, take the two nodes in the boundary of each mesh edge $e \subset \partial T$ and connect them to the centroid of the edge.

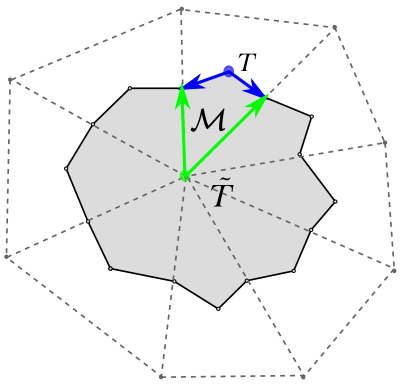

Fig. 1. 2-D example of the fundamental geometric entities involved in the CM formulation.

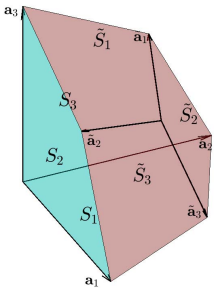

Fig. 2. 3-D fundamental cell.

We note that if $\Omega \subset \mathbb{R}^2$, the facets are already 1-D edges by definition; therefore, one step in procedure can be skipped. In any case, each D-dimensional simplex T of the original mesh is divided into $D+1$ disjoint subsets, which are irregular quadrilaterals for dimension $D = 2$ and irregular hexahedra for $D = 3$. Each of these objects, which we call *fundamental cells* and denote with $\mathcal{M}$ in the rest of the article, is uniquely identified by a pair (T, n), for every mesh vertex $n \subset \partial T$. Subsequently, all fundamental cells $\mathcal{M}$ for which $n \subset \partial \mathcal{M}$ can be agglomerated to obtain a dual cell (a nonconvex polytope) $\tilde{T}$: the usual CM whole dual edges are retrieved by the union of each pair of segments connecting the centroid of a mesh facet to the two barycentra of neighboring simplices.

Fig. 1 shows the result of the procedure for $D = 2$: the primal element T is a triangle and $\tilde{T}$ is the grayed, possibly nonconvex polygon obtained by barycentric subdivision, followed by the appropriate set union of fundamental cells. For $D = 3$ we only show, in Fig. 2, an example of a fundamental cell $\mathcal{M}$, which is always bounded by three quadrilateral surfaces S_1, S_2, S_3 (which are intersections of $\partial \mathcal{M}$ with primal facets of the mesh) and three quadrilateral surfaces $\tilde{S}_1, \tilde{S}_2, \tilde{S}_3$ (which are intersections with the facets of the dual mesh). This kind of partition was already exploited in [10] (to make the method suitable for graphical processing units) and in [9] (to extend the time-domain CM to conductive materials).

We introduce two sets of basis functions for the approximation of the unknown fields

$$\boldsymbol{e}(\boldsymbol{r}, t) = \sum_i^{2N} \hat{u}_i(t) \boldsymbol{w}^i(\boldsymbol{r}), \quad \boldsymbol{h}(\boldsymbol{r}, t) = \sum_i^{2\tilde{N}} \hat{f}_i(t) \tilde{\boldsymbol{w}}^i(\boldsymbol{r}) \tag{5}$$

Authorized licensed use limited to: University of Udine. Downloaded on January 25,2021 at 10:40:43 UTC from IEEE Xplore. Restrictions apply.

where $[\tilde{N}]N$ is the number of oriented [dual] primal edges in the mesh and where new semi-discrete time-dependent DoFs $\hat{u}_i(t)$, $\hat{f}_i(t)$ have been defined. We stress the important factor 2 in the summations' upper limit, which comes from the partition into fundamental cells which indeed splits every primal and dual edge into two disjoint segments of equal length.

The basis functions depend on $\boldsymbol{r}$ but are required to be piecewise uniform in each $\mathcal{M}$, therefore, discontinuous. Nevertheless, if we denote $\mathbf{a}_j$ [$\tilde{\mathbf{a}}_j$] any primal [dual] halved edge, the following properties hold:

$$\boldsymbol{w}^i(\mathcal{M}), \tilde{\boldsymbol{w}}^i(\mathcal{M}) \subset [P^0(\mathcal{M})]^D \quad \forall \mathcal{M}, \tag{6}$$

$$\langle \boldsymbol{w}^i(\mathcal{M}), \mathbf{a}_j \rangle = \delta_{ij}, \quad \langle \tilde{\boldsymbol{w}}^i(\mathcal{M}), \tilde{\mathbf{a}}_j \rangle = \delta_{ij} \tag{7}$$

where $[P^0(\mathcal{M})]^D$ is the space of vector-valued constant functions on $\mathcal{M}$, the inner product is the trivial Euclidean one, and δ_{ij} is the Kronecker delta tensor. Clear dependence on $\boldsymbol{r}$ amounts to dependence on $\mathcal{M}$ and, for both sets of functions only three basis functions do not vanish when we restrict to any $\mathcal{M} \subset \boldsymbol{\Omega}$.

If we take now as reference an arbitrary $\mathcal{M}$, without loss of generality we can use the indices $\{1, 2, 3\}$ for the primal and dual halved edges in $\partial\mathcal{M}$, as shown in Fig. 2. It is then

$$\boldsymbol{w}^i(\mathcal{M}) = \frac{\mathbf{a}_j \times \mathbf{a}_k}{\mathbf{a}_i \cdot \mathbf{a}_j \times \mathbf{a}_k}, \quad \tilde{\boldsymbol{w}}^i(\mathcal{M}) = \frac{\tilde{\mathbf{a}}_j \times \tilde{\mathbf{a}}_k}{\tilde{\mathbf{a}}_i \cdot \tilde{\mathbf{a}}_j \times \tilde{\mathbf{a}}_k}$$

where $\{i, j, k\}$ is any permutation of $\{1, 2, 3\}$. It is trivial to prove through Euclidean geometry that, by virtue of the duality pairing in (7), the $\boldsymbol{w}^i(\mathcal{M})$ have *continuous tangential components* on S_1, S_2, S_3 (or the green oriented edges in the 2-D version), while the $\tilde{\boldsymbol{w}}^i(\mathcal{M})$ have *continuous tangential components* on $\tilde{S}_1, \tilde{S}_2, \tilde{S}_3$ (or, alternatively, the blue edges in the 2-D version). We denote with W [$\tilde{W}$] the linear span of the $\boldsymbol{w}^i(\mathcal{M})$ [$\tilde{\boldsymbol{w}}^i(\mathcal{M})$].

IV. DG FEM Formulation

Starting back again with the continuous problem in (1) and (2), the equations are tested against the basis functions *element-by-element* as in DG-FEM

$$\sum_{\mathcal{M}\subset\boldsymbol{\Omega}} \left(\int_{\mathcal{M}} \varepsilon \partial_t \boldsymbol{e} \cdot \boldsymbol{w} \right) = \sum_{\mathcal{M}\subset\boldsymbol{\Omega}} \left(\int_{\mathcal{M}} \nabla \times \boldsymbol{h} \cdot \boldsymbol{w} \right) \quad \forall \boldsymbol{w} \in W$$

$$\sum_{\mathcal{M}\subset\boldsymbol{\Omega}} \left(\int_{\mathcal{M}} \mu \partial_t \boldsymbol{h} \cdot \tilde{\boldsymbol{w}} \right) = -\sum_{\mathcal{M}\subset\boldsymbol{\Omega}} \left(\int_{\mathcal{M}} \nabla \times \boldsymbol{e} \cdot \tilde{\boldsymbol{w}} \right) \quad \forall \tilde{\boldsymbol{w}} \in \tilde{W}.$$

It easily follows (through integration by parts and the divergence theorem) that:

$$\int_{\mathcal{M}} \nabla \times \boldsymbol{h} \cdot \boldsymbol{w} = \oint_{\partial\mathcal{M}} \boldsymbol{h} \times \boldsymbol{w} \cdot \hat{\boldsymbol{n}}$$

$$\int_{\mathcal{M}} \nabla \times \boldsymbol{e} \cdot \tilde{\boldsymbol{w}} = \oint_{\partial\mathcal{M}} \boldsymbol{e} \times \tilde{\boldsymbol{w}} \cdot \hat{\boldsymbol{n}}$$

where $\hat{\boldsymbol{n}}$ is the outward-pointing unit normal vector on $\partial\mathcal{M}$, and we have also used the fact that the test functions are piecewise uniform. Furthermore, if we finally expand the unknown vector fields in W and $\tilde{W}$, respectively, we get the weak form

$$\sum_{\mathcal{M}\subset\boldsymbol{\Omega}} \int_{\mathcal{M}} \varepsilon \sum_{j=1}^{j=2N} \partial_t \hat{u}_j \boldsymbol{w}^j(\mathcal{M}) \cdot \boldsymbol{w} = \sum_{\mathcal{M}\subset\boldsymbol{\Omega}} \int_{\tilde{S}} \sum_{\ell=1}^{\ell=2\tilde{N}} \hat{f}_\ell \tilde{\boldsymbol{w}}^\ell(\mathcal{M}) \times \boldsymbol{w} \cdot \hat{\boldsymbol{n}}$$

$$\sum_{\mathcal{M}\subset\boldsymbol{\Omega}} \int_{\mathcal{M}} \mu \sum_{\ell=1}^{\ell=2\tilde{N}} \partial_t \tilde{\boldsymbol{w}}^\ell(\mathcal{M}) \cdot \tilde{\boldsymbol{w}} = -\sum_{\mathcal{M}\subset\boldsymbol{\Omega}} \int_{S} \sum_{j=1}^{j=2N} \hat{u}_j \boldsymbol{w}^j(\mathcal{M}) \times \tilde{\boldsymbol{w}} \cdot \hat{\boldsymbol{n}}$$

$\forall \boldsymbol{w} \in W$ and $\forall \tilde{\boldsymbol{w}} \in \tilde{W}$, where $\tilde{S} = \tilde{S}_1 \cup \tilde{S}_2 \cup \tilde{S}_3$ and $S = S_1 \cup S_2 \cup S_3$. Here the staggered partial continuity of the test functions has been exploited to obtain the full semi-discrete formulation. Note that no numerical flux averaging (which is root of spurious solutions in DG approaches) or upwinding (which numerically dissipates energy) is needed.

If we now go back to the reference $\mathcal{M}$, all indices run from 1 to 3 and it can be proved through direct symbolic computation that the 3×3 matrix $\hat{\mathbf{C}}$ whose entry at the i, j position is given by

$$\int_S \boldsymbol{w}^i(\mathcal{M}) \times \tilde{\boldsymbol{w}}^j(\mathcal{M}) \cdot \hat{\boldsymbol{n}} = \int_{\tilde{S}} \boldsymbol{w}^i(\mathcal{M}) \times \tilde{\boldsymbol{w}}^j(\mathcal{M}) \cdot \hat{\boldsymbol{n}}$$

is equal to

$$\hat{\mathbf{C}} = \begin{pmatrix} 0 & 1 & -1 \\ -1 & 0 & 1 \\ 1 & -1 & 0 \end{pmatrix}. \tag{8}$$

It is a (tedious) vector algebra exercise to show that this is valid *on any $\mathcal{M}$ of the mesh up to edge orientation*. This key fact in (8) can also be used to optimize the memory consumption of the algorithm. Indeed, the same $\hat{\mathbf{C}}$ matrix (and its transpose) can be stored once and used for all elements in the mesh. The last step which allows us to retrieve the algebraic form of (3) and (4), as we perform the sums over the whole mesh of the above derived weak form, is to note that physical interpretation of the DoFs has not changed, *halved* line integrals entries have identical r.h.s rows and can be summed back together (with orientation) to retrieve the original discrete geometric interpretation.

V. Numerical Results

We now compare the proposed method with the classic FDTD method and the classic version of the FEM curl-conforming formulation. Time is always discretized using the leapfrog scheme. As a domain $\boldsymbol{\Omega}$, we consider a 3-D metallic rectangular waveguide with cross sections aligned with the xy plane: the authors in [9] have shown that one can obtain a time-domain closed-form solution for the fundamental mode (the TE_{10} mode) impinging at $z = 0$ and encountering a perfectly electric conducting (PEC) termination at a fixed $z = L$.

We can then test convergence by studying the relative errors $\|\epsilon\|$ in the appropriate discrete $\mathbf{L}^2$ norm: Fig. 3 shows,

Authorized licensed use limited to: University of Udine. Downloaded on January 25,2021 at 10:40:43 UTC from IEEE Xplore. Restrictions apply.

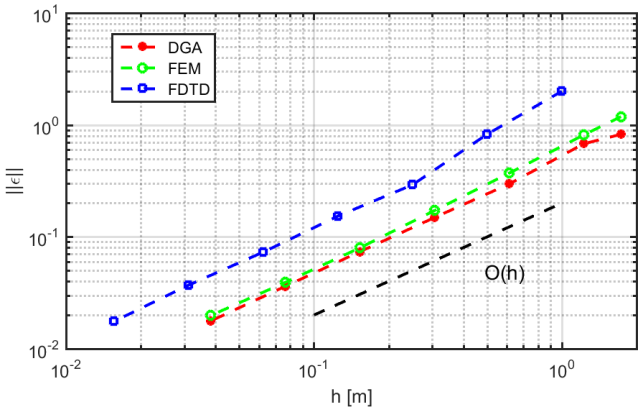

Fig. 3. All the methods tested converge as $\mathcal{O}(h)$ in $\mathbf{L}^2$ norm error, with h being the maximum edge length in the grid.

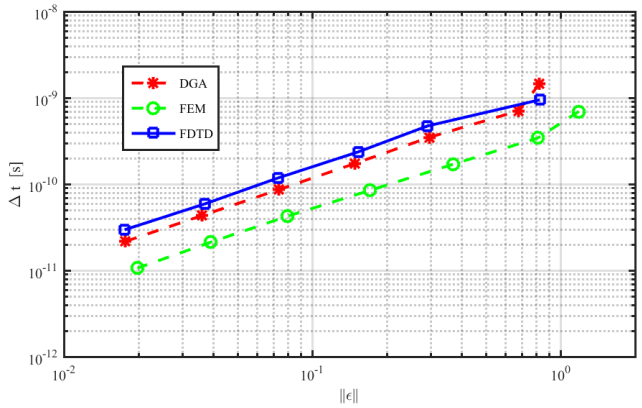

Fig. 4. Log–log plot of the maximum allowed Δt versus the relative accuracy on the test problem for all three methods.

in double logarithmic scales, that the two tetrahedral grid methods are more accurate than the FDTD for grids of comparable size, and all three methods converge linearly with h (average mesh size), i.e., they are exact for piecewise-uniform fields. This last detail is theoretically predicted for the FEM and DGA schemes, and justified for the FDTD (which has theoretically $\mathcal{O}(h^2)$ convergence), through a closer look at the regularity of the closed-form solution (see [9]).

The upper limit value for the time step Δt on successive uniform spatial refinements of the cubic domain for all three methods has also been numerically estimated. To do so, we used the power iteration method to estimate the largest eigenvalue of the discrete evolution matrix. Fig. 4 shows the resulting Δt *versus the accuracy*. Since the time step size is an important factor in computational complexity, the sustained factor 2 between the DGA approach and the FEM approach (for equal accuracy) shows the promise of the proposed method (which we recall is also explicit in time). This empirical result is an original finding of the present contribution, a theoretical study of this behavior for the Courant–Friedrichs–Lewy (CFL) condition is still lacking and goes beyond the scope of this work. Fig. 5, which shows asymptotic computational complexity rates with respect to the measured accuracy of the methods (per time step and for a full simulation) for the same model problem, shows the method is competitive with FDTD (the studied example presents no staircase approximation) and an order of magnitude more efficient than Whitney elements.

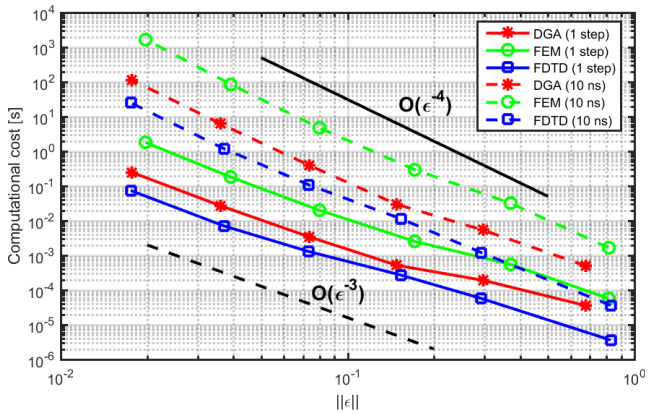

Fig. 5. Log–log plot of the computational cost in seconds versus the relative accuracy on the test problem.

VI. Conclusion

In the present contribution, it was shown that the CM approach in the time-domain solution for Maxwell equations can be entirely recast in the framework of the DG FEM if two lowest order approximations are adopted on staggered barycentric dual meshes, with numerical flux choices made obvious by the partial continuity properties of the basis functions. The present form plows the soil for an extension of the scheme to orders of convergence higher than linear in space, which is currently underway and will be reported in a future submission.

Acknowledgment

The work of B. Kapidani was supported by the Austrian Science Fund (FWF) under Project SFB65.

References

[1] A. Taflove and S. C. Hagness, *Computational Electrodynamics: The Finite-Difference Time-Domain Method*, 2nd ed. Norwood, MA, USA: Artech House, 2000.

[2] J. C. Nedelec, "Mixed finite elements in $\mathbb{R}^3$," *Numer. Math.*, vol. 35, no. 3, pp. 315–341, Sep. 1980.

[3] J.-F. Lee and Z. Sacks, "Whitney elements time domain (WETD) methods," *IEEE Trans. Magn.*, vol. 31, no. 3, pp. 1325–1329, May 1995.

[4] J. S. Hesthaven and T. Warburton, *Nodal Discontinuous Galerkin Methods: Algorithms, Analysis, and Applications*. New York, NY, USA: Springer-Verlag, 2008.

[5] E. Tonti, "Finite formulation of the electromagnetic field," *Prog. Electromagn. Res.*, vol. 32, pp. 1–44, 2001.

[6] L. Codecasa, R. Specogna, and F. Trevisan, "A new set of basis functions for the discrete geometric approach," *J. Comput. Phys.*, vol. 229, no. 19, pp. 7401–7410, 2010.

[7] L. Codecasa and M. Politi, "Explicit, consistent, and conditionally stable extension of FD-TD to tetrahedral grids by FIT," *IEEE Trans. Magn.*, vol. 44, no. 6, pp. 1258–1261, Jun. 2008.

[8] T. Weiland, "Time domain electromagnetic field computation with finite difference methods," *Int. J. Numer. Model., Electron. Netw., Devices Fields*, vol. 9, no. 4, pp. 295–319, Jul. 1996.

[9] L. Codecasa, B. Kapidani, R. Specogna, and F. Trevisan, "Novel FDTD technique over tetrahedral grids for conductive media," *IEEE Trans. Antennas Propag.*, vol. 66, no. 10, pp. 5387–5396, Oct. 2018.

[10] M. Cicuttin, L. Codecasa, B. Kapidani, R. Specogna, and F. Trevisan, "GPU accelerated time-domain discrete geometric approach method for Maxwell's equations on tetrahedral grids," *IEEE Trans. Magn.*, vol. 54, no. 3, Mar. 2018, Art. no. 7203004.

[11] T. Tarhasaari, L. Kettunen, and A. Bossavit, "Some realizations of a discrete Hodge operator: A reinterpretation of finite element techniques," *IEEE Trans. Magn.*, vol. 35, no. 3, pp. 1494–1497, May 1999.

Authorized licensed use limited to: University of Udine. Downloaded on January 25,2021 at 10:40:43 UTC from IEEE Xplore. Restrictions apply.